
	SAKARYA ÜNİVERSİTESİ FEN BİLİMLERİ ENSTİTÜSÜ DERGİSİ <i>SAKARYA UNIVERSITY JOURNAL OF SCIENCE</i>		
	e-ISSN: 2147-835X		
	Dergi sayfası: http://dergipark.gov.tr/saufenbilder		
	<u>Geliş/Received</u> 17-02-2017 <u>Kabul/Accepted</u> 01-06-2017	<u>Doi</u> 10.16984/saufenbilder.292752	

N- ve P-tip Katkılı $Mg_2Si_{1-x}Sn_x$ Katı Alaşımlarının Termal İletkenliklerinin Teorik Çalışması

Övgü Ceyda Yelgel*¹

ÖZ

$Mg_2Si_{1-x}Sn_x$ katı alaşımları yüksek termoelektrik verimlilikleri sebebiyle 500 K'den 800 K'e kadar olan orta sıcaklık aralığı için umut vaadedilen termoelektrik materyallerdir. Bu çalışmada hem n- hem p-tip katkı $Mg_2Si_{1-x}Sn_x$ katı alaşımlarının termal iletkenlikleri teorik olarak detaylıca incelenmesi sunulmuştur. Taşıyıcılardan (elektronlar yada holler), elektron-hole çiftlerinden ve fononlardan kaynaklanan termal iletkenlik katkıları ayrı ayrı göz önüne alınarak ve sırasıyla Wiedeman-Franz kanunu, Price'in teorisi, ve Debye'nin izotropik sürekli modeli uygulanarak hesaplanmıştır. Bütün fonon çarpışma mekanizmaları, kaynağı kristal sınırlarından, kütle bozukluklarından, bozunum potansiyellerinden ve anharmoniklikten olan katı alaşımların hepsi için eksiksiz bir şekilde incelenmiştir. En düşük toplam termal iletkenlik değerleri n-tip katkı $Mg_2(Si_{0.4}Sn_{0.6})_{0.98}Bi_{0.02}$ katı alaşım için 700 K'de $2.431 \text{ WK}^{-1}\text{m}^{-1}$ olarak, p-tip katkı $Mg_2(Si_{0.3}Sn_{0.7})_{0.95}Ga_{0.05}$ katı alaşım için 600 K'de $1.843 \text{ WK}^{-1}\text{m}^{-1}$ olarak bulunmuştur buda açıkça öneriyor ki p-tip katkı $Mg_2Si_{1-x}Sn_x$ tabanlı katı alaşımlar n-tip katkı katı alaşımlarından termoelektrik cihazlar için daha iyi adaylardır.

Anahtar kelimeler: termoelektrik materyaller, termal iletkenlik, fonon termal iletkenlik

Theoretical Study of Thermal Conductivities of n- and p-type Doped $Mg_2Si_{1-x}Sn_x$ Thermoelectric Solid Solutions

ABSTRACT

$Mg_2Si_{1-x}Sn_x$ solid solutions are a promising class of thermoelectric materials due to their high thermoelectric efficiencies at intermediate temperature range from 500 K to 800 K. Present study presents a theoretical work of the thermal conductivities of both n- and p-type doped $Mg_2Si_{1-x}Sn_x$ solid solutions. The thermal conductivity contributions arising from carriers (electrons or holes), electron-hole pairs, and phonons are taken into account separately by employing the Wiedemann-Franz law, Price's theory, and Debye's isotropic continuum model, respectively. All phonon scattering mechanisms originate from crystal boundaries, mass-defects, deformation potentials, and anharmonicity are investigated rigorously for all solid solutions. The lowest total thermal conductivity values are obtained as $2.431 \text{ WK}^{-1}\text{m}^{-1}$ at 700 K for n-type doped $Mg_2(Si_{0.4}Sn_{0.6})_{0.98}Bi_{0.02}$ solid solution and $1.843 \text{ WK}^{-1}\text{m}^{-1}$ at 600 K for p-type doped $Mg_2(Si_{0.3}Sn_{0.7})_{0.95}Ga_{0.05}$ solid solution which clearly suggest that p-type doped $Mg_2Si_{1-x}Sn_x$ based solid solutions are better candidates for the thermoelectric devices than their n-type doped solid solutions.

Keywords: thermoelectric materials, thermal conductivity, phonon thermal conductivity

¹ Recep Tayyip Erdoğan Üniversitesi, Mühendislik Fakültesi, Malzeme Bilimi ve Nanoteknoloji Bölümü, Rize – oceyda.yelgel@erdogan.edu.tr

1. INTRODUCTION

Thermoelectric devices can transform thermal gradients to electricity and vice versa. Both thermoelectric generators and refrigerators are used for waste heat recovery. A thermoelectric device has many advantages such as they have no moving parts, have long term lifetime, are non-toxic, are noise and pollution free and are made from elements that are abundant in nature. Thermoelectric energy conversion efficiency is determined by the dimensionless thermoelectric figure of merit given by the equation as

$$ZT = \frac{S^2 \sigma}{\kappa_{total}} T, \quad (1)$$

where S is the Seebeck coefficient (V/K), σ is the electrical conductivity (S/m), T is the absolute temperature (K), and κ_{total} is the total thermal conductivity (W/m.K) consists three different contributions from carriers (electrons or holes; κ_c), from electron-hole pairs (κ_{bp}), and from phonons (κ_{ph}). An ideal, practical thermoelectric device should at least have a value of $ZT > 1$ which leads about 10% conversion efficiency. To achieve a higher ZT has always been the motivation for the research of thermoelectric research area, however, due to strong interrelation of thermoelectric parameters S , σ , and κ_{total} , improving one leads to simultaneous deterioration of other two parameters. The common approach to improve ZT for bulk materials is making alloys with the formation of point defects by substitutional doping. This is the most general way to improve the power factor ($S^2\sigma$) by optimisation of carrier concentration and/or reduce the phonon thermal conductivity due to improving point defect scattering originates from the mass difference between host atoms and dopants [1]. One of the best thermoelectric materials are highly doped semiconductors since heat is carried predominantly by phonons thus the total thermal conductivity is largely decoupled from the power factor [1]. Among these doped semiconductors alkaline earth metal silicides Mg_2X ($X=Si, Ge, \text{ and } Sn$) are class of materials generally used for thermoelectric device applications in the intermediate temperature range from 500 K to 800 K due to (1) relative abundance, (2) thermal stability, (3) non-toxicity, and (4) low cost of production and environment friendly [1]. These intermetallic Mg_2X

compounds have been well known for the applications of automobiles and aerospace industry due to their high specific elastic modulus [2]. Mg_2X compounds are narrow band gap semiconductors and have a face-centred cubic (FCC) structure with primitive translation vectors $a = a(0, 1/2, 1/2)$, $b = a(1/2, 0, 1/2)$, and $c = a(1/2, 1/2, 0)$ where a is the lattice parameter. At ambient conditions, Mg_2X crystallizes in cubic antiferrotype structure with space group $Fm\bar{3}m$ with one molecular unit per primitive cell and four formulas per fcc conventional cell [3], as represented in Fig. 1. Sufficiently high values of ZT for these Mg_2X ($X=Si, Ge, \text{ and } Sn$) based compounds were found in the literature [4]–[7]. The ZT value of undoped Mg_2Si was found to be $ZT = 0.04\text{--}0.06$ at nearly 750 K [8]–[10] while this could be significantly enhanced by doping with Sn, Ge, Sb, and Bi. As an example, very high value of thermoelectric figure of merit was gained for $Mg_2Si_{0.6}Sn_{0.4}$ as $ZT_{max}=1.2$ at 700 K [11] and for $Mg_2Si_{0.53}Sn_{0.4}Ge_{0.05}Bi_{0.02}$ as $ZT_{max}=1.4$ at 823 K [12].

Here thermal conductivities of n-type doped $Mg_2(Si_{0.4}Sn_{0.6})_{1-y}Bi_y$ where $y=0.02$ and 0.03 and p-type doped $Mg_2(Si_{0.3}Sn_{0.7})_{1-y}Ga_y$ where $y=0.05$ and 0.07 solid solutions is reported theoretically in temperature range between 300 K and 800 K. All thermal transport properties including contributions from carriers (namely donor electrons for n-type doped samples and acceptor holes for p-type doped samples) (κ_c), electron-hole pairs (κ_{bp}), and phonons (κ_{ph}) are calculated separately to compare the κ_{total} results of both type doped samples. The Wiedemann-Franz law, Price's theory [13], and Srivastava's scheme [14] are employed to calculate κ_c , κ_{bp} , and κ_{ph} , respectively. All phonon scattering mechanisms including boundary scattering, mass-defect scattering,

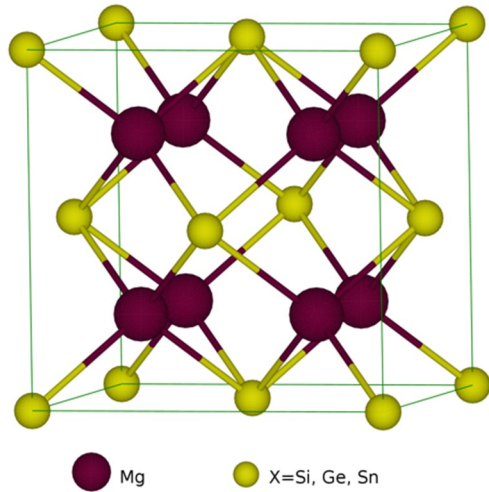


Figure 1 The cubic anti-fluorite type crystal structure of Mg₂X (X=Si, Ge, Sn).

acoustic deformation potential scattering, and anharmonic phonon scattering are taken into account rigorously. Furthermore the percentage contributions from different polarisations (longitudinal and transverse) towards the phonon thermal conductivity are presented for all types of samples.

2. THEORY

The total thermal conductivity of semiconductor materials ($\kappa_{total} = \kappa_c + \kappa_{bp} + \kappa_{ph}$) has included three contributions from carriers (electrons for n-type, holes for p-type), electron-hole pairs (bipolar), and phonons, respectively.

2.1. Carrier Thermal Conductivity

By using Wiedemann-Franz law the carrier thermal conductivity is written as [15]

$$\kappa_c = \sigma \mathcal{L} T = \left(\frac{k_B}{e}\right)^2 \sigma T \mathcal{L}_0, \quad (1)$$

where k_B is the Boltzmann constant, \mathcal{L} is the Lorenz number and the expression of \mathcal{L}_0 is given by

$$\mathcal{L}_0 = \frac{\left(\frac{r+7}{2}\right) F_{\frac{r+5}{2}}(\zeta^*)}{\left(\frac{r+3}{2}\right) F_{\frac{r+1}{2}}(\zeta^*)} - \left[\frac{\left(\frac{r+5}{2}\right) F_{\frac{r+3}{2}}(\zeta^*)}{\left(\frac{r+3}{2}\right) F_{\frac{r+1}{2}}(\zeta^*)} \right]^2, \quad (2)$$

where Fermi integral is given as $F_i = \int_0^\infty x^i \frac{dx}{e^{(x-\zeta^*)} + 1}$ for bulk semiconductor materials [16].

In doped semiconductors, carriers generally scatter with the long wave-length phonons which means that the most important phonon scattering mechanism is sourced from acoustic phonon scattering [17], [18]. Thus, in the extrinsic regime the electrical conductivity of semiconductors is given by [19]

$$\sigma_{ext} = \frac{4}{3\pi\sqrt{\pi}} \frac{e^2}{m_c^*} \frac{\hbar \rho c_L^2}{E_D^2} F_{1/2}, \quad (3)$$

where m_c^* is the carrier's conductivity effective mass, c_L is the velocity of longitudinal phonons, ρ is the mass density, and E_D is the deformation potential. In addition to hole acoustic phonon scattering there is also additional scattering mechanisms occur in electrical conductivity. So that, with the inclusion of these additional mechanisms the electrical conductivity can be scaled as

$$\sigma_{extrinsic} = \sigma_{ext} A T^\zeta \quad (4)$$

with A and ζ being adjustable parameters. Electrical conductivity in the intrinsic regime can be re-defined by using Wilson's expression as [20]

$$\sigma_{int} = A' e^{-E_g/2k_B T}, \quad (5)$$

where A' is a temperature invariant parameter. Similar to $\sigma_{extrinsic}$, due to the additional free carrier-phonon scattering in the intrinsic regime the electrical conductivity can be re-expressed as

$$\sigma_{intrinsic} = 1/\sigma_{int} + A T, \quad (6)$$

where A' is treated as an adjustable parameter. The band gap E_g temperature variation of n-type doped semiconductors is given as [21]

$$E_g(T) = E_g(0) - \alpha T, \quad (7)$$

and for p-type doped semiconductors is written as by following Yelgel's formula [22]

$$E_g(T) = \left[E_g(0) - \frac{\alpha T^2}{\beta + T} \right] + \frac{\eta T}{\beta + T}, \quad (8)$$

where $E_g(0)$ is the value of E_g at 0 K, and α , β , and η are treated as adjustable parameters.

2.2. Bipolar Thermal Conductivity

Mg₂X compounds have small band gaps in which the bipolar thermal conductivity becomes significant only above 300 K, its expression is given by [13]

$$\kappa_{bp} = F_{bp} T^{\zeta} \exp(-E_g/2 k_B T), \quad (9)$$

where E_g is a band gap of a material, F_{bp} and ζ regarded as adjustable parameters.

2.3. Phonon Thermal Conductivity

Using Debye’s isotropic continuum model within the single-mode relaxation time approximation the phonon thermal conductivity is given as [14]

$$\kappa_{ph} = \frac{\hbar^2 q_D^5}{6\pi^2 k_B T^2} \sum_s c_s^4 \int_0^1 dx x^4 \tau \bar{n}(\bar{n} + 1), \quad (10)$$

where τ is the phonon relaxation time, q_D is the Debye radius, $x = q/q_D$ is a reduced wavenumber, s represents the polarisation branch of phonon (longitudinal or transverse), n is the Bose-Einstein distribution function, and c_s is the velocity of phonons for polarisation branch s . The phonon relaxation rate (τ^{-1}) is contributed by several scattering mechanisms and by using the Matthiessen rule the total effect of scattering processes is defined as $\tau^{-1} = \sum_i \tau_i^{-1}$, where τ_i^{-1} represents the contribution from i^{th} scattering mechanism. The scattering mechanisms can be summarised as in the following forms.

Boundary scattering: When phonons interact with the boundaries of a sample the scattering mechanism is defined as

$$\tau_{qs}^{-1}(bs) = \frac{c_s}{L}, \quad (11)$$

where L is a crystal size [14], [23].

Mass defect scattering: The scattering of phonons from isotopes and alloying in semiconductor alloys and compounds is written as [14], [24]

$$\tau_{qs}^{-1} = \frac{\Gamma_{md} \Omega}{4\pi \bar{c}^3} w^4(qs), \quad (12)$$

where Ω is the volume of a unit cell, \bar{c} is the average phonon velocity, $w=cq$ and Γ_{md} is the mass-defect parameter. For a single-species crystal, the isotopic mass-defect parameter takes the form [24]

$$\Gamma_{isotopes} = \sum_i f_i \left(\frac{\Delta M_i}{\bar{M}} \right)^2, \quad (13)$$

where f_i is the percentage of i^{th} isotope present in the crystal and $\Delta M_i = M_i - \bar{M}$, with \bar{M} is the average atomic mass. For a composite material, such as an alloy, with molecular formula $A_x B_y C_z \dots$ the mass-defect parameter is given by [24]

$$\begin{aligned} \Gamma_{alloy}(A_x B_y C_z \dots) &= \frac{x}{(x+y+z+\dots)} \left(\frac{M_A}{\bar{M}} \right)^2 \Gamma(A) \\ &+ \frac{y}{(x+y+z+\dots)} \left(\frac{M_B}{\bar{M}} \right)^2 \Gamma(B) \\ &+ \frac{z}{(x+y+z+\dots)} \left(\frac{M_C}{\bar{M}} \right)^2 \Gamma(C) + \dots, \quad (14) \end{aligned}$$

where $\Gamma(A) = \sum_{(i)} f_i \left(\frac{\Delta M_i(A)}{\bar{M}_A} \right)^2$ represents the defect parameter for atomic species A , and the average atomic mass is expressed as $\bar{M} = (xM_A + yM_B + zM_C + \dots)/(x + y + z + \dots)$.
Acoustic deformation potential scattering: The scattering of charge carriers (electrons for n-type samples, holes for p-type samples) with acoustic mode phonons is expressed as [25]

$$\tau_{ql}^{-1}(dp) = \frac{3}{8\sqrt{\pi}} \frac{E_{df}^2}{\rho c^2 \hbar^4} (2m_c^* k_B T)^{3/2}, \quad (14)$$

where E_{df} is a scaled deformation potential.

Anharmonic phonon scattering: By restricting ourselves to only three phonon processes and following Srivastava’s scheme [14] the phonon-phonon scattering mechanism is given by

$$\begin{aligned} \tau_{qs}^{-1}(anh) &= \frac{\hbar q_D^5 \gamma^2}{4\pi \rho \bar{c}^2} \sum_{s's''\epsilon} \left[\int dx' x'^2 x'' \left[(1 - \right. \right. \\ &\quad \left. \left. \epsilon + \epsilon(C_x + Dx') \right) \right] + \frac{1}{2} \int dx' x'^2 x'' \left[(1 - \right. \right. \\ &\quad \left. \left. \epsilon + \epsilon(C_x + Dx') \right) \right] \frac{n_{qs}^+ (n_{qs}^-)}{n_{qs}} \right], \quad (15) \end{aligned}$$

where γ is the Grüneisen constant, $x' = q'/q_D$, $x'' = Cx \pm Dx'$, $n_{\pm} = n(x_{\pm})$, $C = c_s/c_{s''}$, $D = c_s'/c_{s''}$. $\epsilon = 1$ for momentum-conserving processes and $\epsilon = -1$ for momentum-nonconserving processes. The first and second terms in Eq. (17) are controlled by class 1 events ($qs + q's'' \rightarrow q''s''$) and class 2 events ($qs \rightarrow q's' + q''s''$), respectively. The integration limits on the variables x and x' have already been given in Ref. [14].

3. RESULTS AND DISCUSSION

Thermal conductivities are performed for n-type doped $Mg_2(\text{Si}_{0.4}\text{Sn}_{0.6})_{1-y}\text{Bi}_y$ ($y=0.02$ and 0.03) and p-type doped $Mg_2(\text{Si}_{0.3}\text{Sn}_{0.7})_{1-y}\text{Ga}_y$ ($y=0.05$ and 0.07) solid solutions in the temperature range $300 \text{ K} \leq T \leq 800 \text{ K}$. All the required properties and parameters are listed in Tab. 1.

The carrier thermal conductivities of both type doped solid solutions are calculated and represented in Fig. 2.

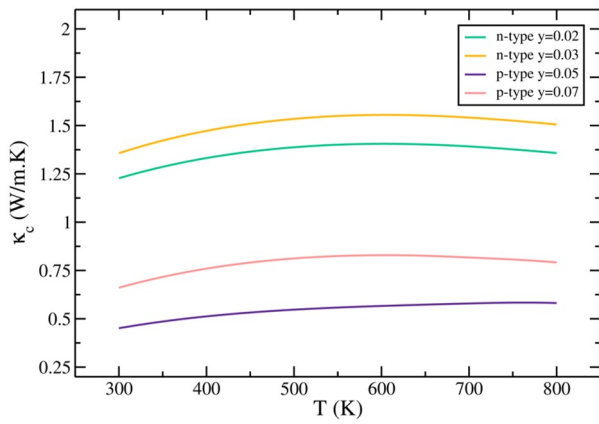


Figure 2 Temperature dependence of carrier thermal conductivity for n-type doped Mg₂(Si_{0.4}Sn_{0.6})_{1-y}Bi_y (y=0.02 and 0.03) solid solutions and p-type doped Mg₂(Si_{0.3}Sn_{0.7})_{1-y}Ga_y (y=0.05 and 0.07) solid solutions.

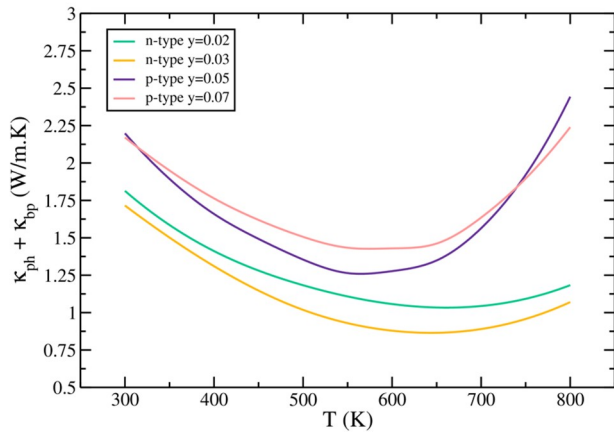


Figure 3 Temperature dependence of the sum of phonon and bipolar thermal conductivity for n-type doped Mg₂(Si_{0.4}Sn_{0.6})_{1-y}Bi_y (y=0.02 and 0.03) solid solutions and p-type doped Mg₂(Si_{0.3}Sn_{0.7})_{1-y}Ga_y (y=0.05 and 0.07) solid solutions.

For both n- and p-type doped samples κ_c goes up with higher doping level because of rise in the electrical conductivity as the doping level increases. The reason of significantly lower κ_c values for p-type doped samples originates from their lower electrical conductivities both with their smaller Lorenz numbers and band gap values compared to n-type doped samples. Additionally, from our theoretical calculations it is found that for both n- and p-type doped samples throughout the temperature range κ_c increases with temperature smoothly. The theoretical calculation of the sum of phonon and bipolar thermal conductivities for both type doped samples are shown in Fig. 3. From our theoretical calculations it is found that for both type doped samples boundary and carrier-phonon scatterings are

important at temperatures below 100 K, the anharmonic phonon scattering is important at temperatures above 100 K and mass-defect scatterings become significant both at low and high temperatures. Additionally, it is found theoretically that for both type samples κ_{bp} increases exponentially with temperature and it becomes significant for n-type doped samples above 550 K while for p-type doped samples above 650 K. The increment in κ_{bp} from 500 K to 800 K is faster for n-type doped samples than p-type doped samples. Moreover, from our theoretical calculations the smaller values of κ_{bp} is gained for p-type doped samples due to their smaller energy band gaps at. Finally, as shown in Fig. 3 n-type doped samples have lower $\kappa_{ph} + \kappa_{bp}$ values than p-type doped samples the reason for this is even n-type doped samples have higher κ_{bp} values they have lower κ_{ph} values due to their larger mass-defect scatterings defined by Γ_{md} parameters as listed in Tab. The temperature variation of the percentage contribution from different polarisations of phonon thermal conductivity for both n- and p-type doped samples is presented in Fig. 4 and Fig. 5, respectively.

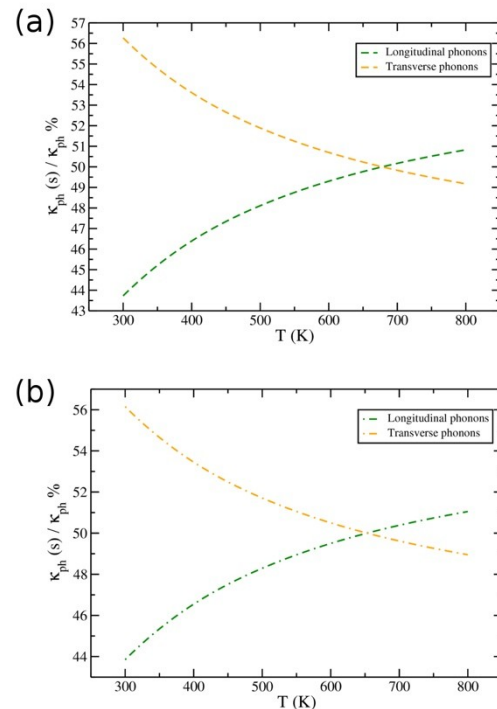


Figure 4 Temperature variation of the percentage contribution from different polarisations of phonon thermal conductivity for n-type doped Mg₂(Si_{0.4}Sn_{0.6})_{1-y}Bi_y (y=0.02 and 0.03) solid solutions.

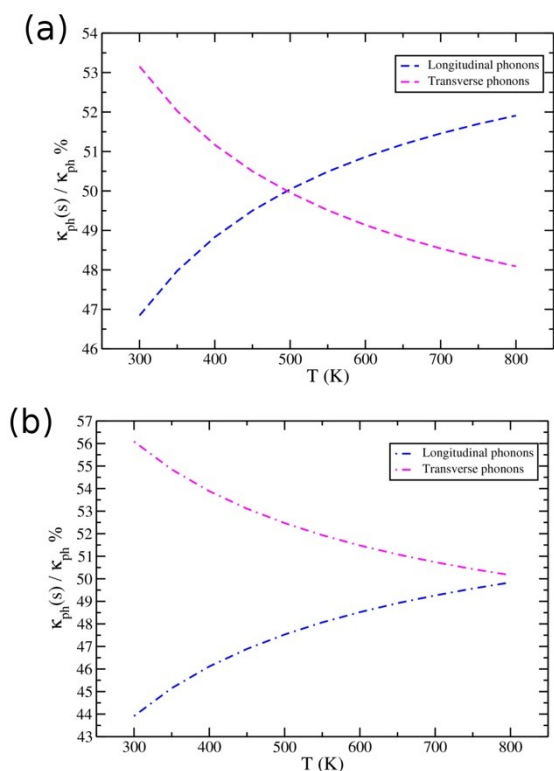


Figure 5 Temperature variation of the percentage contribution from different polarisations of phonon thermal conductivity for p-type doped Mg₂(Si_{0.3}Sn_{0.7})_{1-y}Ga_y (y=0.05 and 0.07) solid solutions.

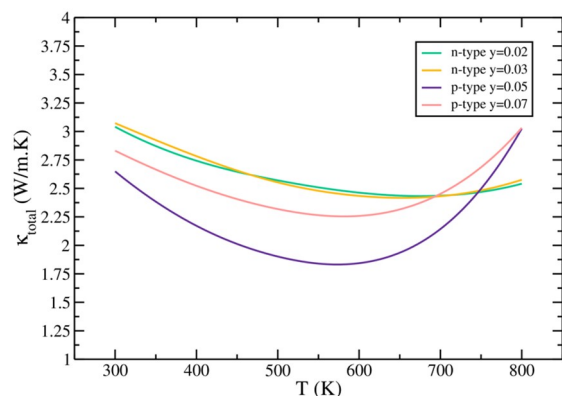


Figure 6 Temperature dependence of total thermal conductivity for n-type doped Mg₂(Si_{0.4}Sn_{0.6})_{1-y}Bi_y (y=0.02 and 0.03) solid solutions and p-type doped Mg₂(Si_{0.3}Sn_{0.7})_{1-y}Ga_y (y=0.05 and 0.07) solid solutions.

For n-type doped samples, shown in Fig. 4, while the phonon thermal conductivity is carried by transverse phonons with nearly 56 % at 300 K this decreases with temperature and after reaching at critical temperature ($T_c=690$ K and $T_c=650$ K for y=0.02 sample and y=0.03 sample, respectively) heat mostly carried by by longitudinal phonons with 51 %. For p-type doped Mg₂(Si_{0.3}Sn_{0.7})_{0.95}Ga_{0.05} sample at temperatures

below 500 K while the phonon thermal conductivity is carried by transverse phonons with 53 % after that critical temperature κ_{ph} is carried dominantly by longitudinal phonons with %52.

On the other hand, being different from other three samples in p-type doped Mg₂(Si_{0.3}Sn_{0.7})_{0.93}Ga_{0.07} solid solution heat is mostly carried by transverse phonons throughout the temperature range 300 K to 800 K. The total thermal conductivities of both type doped samples are demonstrated in Fig. 6. From the theoretical calculations the lower values of κ_{total} is gained for p-type doped samples due to their significantly smaller carrier thermal conductivities whereas they have lower phonon thermal conductivities than n-type doped samples. The lowest value of κ_{total} is found to be for p-type doped Mg₂(Si_{0.3}Sn_{0.7})_{0.95}Ga_{0.05} solid solution as 1.843 WK⁻¹m⁻¹ at 600 K whereas the lowest κ_{total} value for n-type doped sample is gained for n-type doped Mg₂(Si_{0.4}Sn_{0.6})_{0.97}Bi_{0.03} solid solution as 2.431 WK⁻¹m⁻¹ at 700 K. These findings clearly suggest that by using p-type doped Mg₂Si_{1-x}Sn_x based solid solutions instead of their n-type doped types are likely to enhance the value of thermoelectric figure of merit.

4. CONCLUSION

The theoretical study of the three different thermal conductivity contributions (sourced from carriers (electrons or holes), electron-hole pairs, and phonons) for n-type doped Mg₂(Si_{0.4}Sn_{0.6})_{1-y}Bi_y with y=0.02 and 0.03 and p-type doped Mg₂(Si_{0.3}Sn_{0.7})_{1-y}Ga_y with y=0.05 and 0.07 solid solutions is presented in the temperature range 300 K ≤ T ≤ 800 K. The following conclusions can be made from our theoretical investigations;

- (1) The lowest carrier thermal conductivities are found to be 1.227 WK⁻¹m⁻¹ at 300 K for n-type doped Mg₂(Si_{0.4}Sn_{0.6})_{0.98}Bi_{0.02} sample and 0.451 WK⁻¹m⁻¹ at 300 K for p-type doped Mg₂(Si_{0.3}Sn_{0.7})_{0.95}Ga_{0.05} sample.
- (2) The smallest values of $\kappa_{ph} + \kappa_{bp}$ are gained as 0.879 WK⁻¹m⁻¹ at 600 K for n type doped Mg₂(Si_{0.4}Sn_{0.6})_{0.97}Bi_{0.03} sample and 1.277 WK⁻¹m⁻¹ at 600 K for p type doped Mg₂(Si_{0.3}Sn_{0.7})_{0.95}Ga_{0.05} sample.

(3) For an efficient thermoelectric material one needs to have smaller κ_{total} value. In this theoretical study significantly lower total thermal conductivity values are gained for both n- and p-type doped Mg₂Si_{1-x}Sn_x based solid solutions. The lowest κ_{total} values are obtained as 2.431 WK⁻¹m⁻¹ at 700 K for n-type doped Mg₂(Si_{0.4}Sn_{0.6})_{0.98}Bi_{0.02} sample and 1.843 WK⁻¹m⁻¹ at 600 K for p-type doped Mg₂(Si_{0.3}Sn_{0.7})_{0.95}Ga_{0.05} sample. This result suggests that p-type doped Mg₂Si_{1-x}Sn_x based solid solutions are better candidates for the thermoelectric devices than their n-type doped solid solutions.

Table 1: Related parameters employed in the computation of thermoelectric properties of n-type doped Mg₂(Si_{0.4}Sn_{0.6})_{1-y}Bi_y where y=0.02 and 0.03 and p-type doped Mg₂(Si_{0.3}Sn_{0.7})_{1-y}Ga_y where y=0.05 and 0.07 solid solutions.

	n-type		p-type	
	y=0.02	y=0.03	y=0.05	y=0.07
E _g (0) (eV)[26]	0.62	0.62	0.476	0.476
α(eV/K)	0.00087	0.000885	0.0011	0.0013
β (K)	—	—	14	14
η (eV)	—	—	0.32	0.32
ρ (kg/m ³)[26]	2.906x10 ³	2.906x10 ³	3.077x10 ³	3.077x10 ³
C _L (m/s)[26]	6.606x10 ³	6.606x10 ³	5.79x10 ³	5.79x10 ³
m _c [*] /m _e [*]	2.28	2.286	1.78	1.68
E _D (eV)	0.17	0.2	8.265	8.265
A (K ⁻¹)	0.1706	0.1730	0.038	0.022
A' (ohm.m.K ⁻¹)	1.0x10 ⁻⁴	1.0x10 ⁻⁴	2.05x10 ⁻⁵	2.05x10 ⁻⁵
A'' (ohm.m.K ⁻¹)	1.56x10 ⁻⁸	1.4x10 ⁻⁸	3.9x10 ⁻⁸	2.9x10 ⁻⁸
F _{bp} (Wm ⁻¹ K ⁻²)	4.0x10 ⁻⁴	3.5x10 ⁻⁴	1.7x10 ⁻⁴	0.48x10 ⁻⁴
a _{lat} (Å)	6.59	6.59	6.63	6.63
ζ	1	1	1	1
q _D (Å ⁻¹)[26]	0.938	0.938	0.9326	0.9326
L (mm)	10	10	0.2	0.2
Ω(Å ³)	73.254	73.254	73.254	73.254
Γ _{md}	2.628x10 ⁻³	3.285x10 ⁻³	6.44x10 ⁻⁴	7.72x10 ⁻⁴
E _{df} (eV)	0.17	0.2	0.202	0.146
γ [27]	1.4	1.4	1.4	1.4

ACKNOWLEDGEMENTS

This work was supported both by the Scientific Research Projects Coordination Unit of Recep Tayyip Erdoğan University with the project

id:373 and project code:2016.53007.109.06.01 and by Scientific and Technical Research Council of Turkey (TÜBİTAK) with the grant number of 115F387.

REFERENCES

[1] V. K. Zaitsev, M. I. Fedorov, I. S. Eremin, E. A. Gurieva, and D. M. Rowe, ‘Thermoelectrics handbook: macro to nano’, *CRC Press. Taylor Fr. Boca Rat.*, 2006.

[2] C. Li, Y. Wu, H. Li, and X. Liu, ‘Microstructural formation in hypereutectic Al-Mg₂Si with extra Si’, *J. Alloys Compd.*, vol. 477, no. 1, pp. 212–216, 2009.

[3] P. M. Lee, ‘Electronic structure of magnesium silicide and magnesium germanide’, *Phys. Rev.*, vol. 135, no. 4A, p. A1110, 1964.

[4] S. K. Bux, M. T. Yeung, E. S. Toberer, G. J. Snyder, R. B. Kaner, and J.-P. Fleurial, ‘Mechanochemical synthesis and thermoelectric properties of high quality magnesium silicide’, *J. Mater. Chem.*, vol. 21, no. 33, pp. 12259–12266, 2011.

[5] V. K. Zaitsev *et al.*, ‘Highly effective Mg₂Si_{1-x}Sn_x thermoelectrics’, *Phys. Rev. B*, vol. 74, no. 4, p. 45207, 2006.

[6] X. Liu *et al.*, ‘Low electron scattering potentials in high performance Mg₂Si_{0.45}Sn_{0.55} based thermoelectric solid solutions with band convergence’, *Adv. Energy Mater.*, vol. 3, no. 9, pp. 1238–1244, 2013.

[7] W. Liu *et al.*, ‘High figure of merit and thermoelectric properties of Bi-doped Mg₂Si_{0.4}Sn_{0.6} solid solutions’, *J. Solid State Chem.*, vol. 203, pp. 333–339, 2013.

[8] T. Dasgupta, C. Stiewe, R. Hassdorf, A. J. Zhou, L. Boettcher, and E. Mueller, ‘Effect of vacancies on the thermoelectric properties of Mg₂Si_{1-x}Sb_x (0 ≤ x ≤ 0.1)’, *Phys. Rev. B*, vol. 83, no. 23, p. 235207, 2011.

[9] J.-Y. Jung, K.-H. Park, and I.-H. Kim, ‘Thermoelectric Properties of Sb-doped Mg₂Si Prepared by Solid-State Synthesis’, *IOP Conf. Ser. Mater. Sci. Eng.*, vol. 18, no. 14, p. 142006, 2011.

- [10] J. Tani and H. Kido, ‘Thermoelectric properties of Sb-doped Mg₂Si semiconductors’, *Intermetallics*, vol. 15, no. 9, pp. 1202–1207, 2007.
- [11] M. I. Fedorov, V. K. Zaitsev, and G. N. Isachenko, ‘High effective thermoelectrics based on the Mg₂Si-Mg₂Sn solid solution’, *Solid State Phenomena*, 2011, vol. 170, pp. 286–292.
- [12] A. U. Khan, N. Vlachos, and T. Kyratsi, ‘High thermoelectric figure of merit of Mg₂Si_{0.55}Sn_{0.4}Ge_{0.05} materials doped with Bi and Sb’, *Scr. Mater.*, vol. 69, no. 8, pp. 606–609, 2013.
- [13] P. J. Price, ‘CXXXV. Ambipolar thermodiffusion of electrons and holes in semiconductors’, *London, Edinburgh, Dublin Philos. Mag. J. Sci.*, vol. 46, no. 382, pp. 1252–1260, 1955.
- [14] G. P. Srivastava, ‘*The physics of phonons*’, CRC press, 1990.
- [15] D. M. Rowe, ‘Thermoelectrics handbook: macro to nano’, *Thermoelectr. Handb. Macro to Nano*, vol. 80, no. 10, p. 1014, 2005.
- [16] R. R. Heikes and R. W. Ure, ‘*Thermoelectricity: science and engineering*’, Interscience Publishers, 1961.
- [17] J. Tani and H. Kido, ‘Thermoelectric properties of Bi-doped Mg₂Si semiconductors’, *Phys. B Condens. Matter*, vol. 364, no. 1, pp. 218–224, 2005.
- [18] T. Yi *et al.*, ‘Synthesis and characterization of Mg₂Si/Si nanocomposites prepared from MgH₂ and silicon, and their thermoelectric properties’, *J. Mater. Chem.*, vol. 22, no. 47, pp. 24805–24813, 2012.
- [19] Ö. C. Yelgel and G. P. Srivastava, ‘Thermoelectric properties of n-type Bi₂(Te_{0.85}Se_{0.15})₃ single crystals doped with CuBr and SbI₃’, *Phys. Rev. B*, vol. 85, no. 12, p. 125207, 2012.
- [20] A. H. Wilson, ‘The Theory of Metals Cambridge’, *Gt. Britain*, p. 26, 1953.
- [21] J. P. McKelvey, ‘Solid state and semiconductor physics’, 1966.
- [22] Ö. Ceyda Yelgel and G. P. Srivastava, ‘Thermoelectric properties of p-type (Bi₂Te₃)_x(Sb₂Te₃)_{1-x} single crystals doped with 3 wt.% Te’, *J. Appl. Phys.*, vol. 113, no. 7, p. 73709, 2013.
- [23] G. S. Nolas, H. J. Goldsmid, and T. M. Tritt, ‘Thermal Conductivity: Theory, Properties, and Applications’, 2004.
- [24] M. G. Holland, ‘Phonon scattering in semiconductors from thermal conductivity studies’, *Phys. Rev.*, vol. 134, no. 2A, p. A471, 1964.
- [25] M. Grundmann, ‘The Physics of Phonons: An Introduction Including Devices and Nanophysics’. Springer, Berlin, 2006.
- [26] O. Madelung, U. Rössler, and M. Schulz, ‘Non-tetrahedrally bonded elements and binary compounds I’, *Landolt-Börnstein Ser.*, vol. 3, 1998.
- [27] H. Wang, H. Jin, W. Chu, and Y. Guo, ‘Thermodynamic properties of Mg₂Si and Mg₂Ge investigated by first principles method’, *J. Alloys Compd.*, vol. 499, no. 1, pp. 68–4, 2010.